ROYAL SOCIETY OF CHEMISTRY

PAPER

Check for updates

Strong chiroptical properties from thin films of chiral imidazole derivatives allowing for easy detection of circularly polarized luminescence†

Andrea Taddeucci, [ID] ‡ Caterina Campinoti, [ID] ‡ Francesca Sardelli, Gennaro Pescitelli, [ID] Lorenzo Di Bari, [ID] Marco Lessi [ID] * and Francesco Zinna [ID] *

We report the synthesis and characterization of four similar chiral 1-methyl-1*H*-imidazole π-conjugated derivatives. In particular, we focus on the thin film chiroptical characterization (electronic circular dichroism and circular polarized luminescence), able to highlight how small changes in the chemical structure can lead to significant variations in the solid state aggregation. For one material showing relevant circularly polarized luminescence (CPL) properties, we have been able to detect the signal with the aid of an ultra-cheap setup we designed, which in this case showed good performance in comparison to our standard CPL instrument. We demonstrated that this setup can detect CPL signals with elevated dissymmetry factor in spite of its highly reduced complexity and much lower cost if compared to conventional CPL instrumentations.

Introduction

In the last few years, organic π-conjugated molecules have been widely adopted in electronics,[1,2] extending their scope to a field

Dipartimento di Chimica e Chimica Industriale, Università di Pisa, via Moruzzi 13, 56124, Pisa, Italy. E-mail: marco.lessi@unipi.it, francesco.zinna@unipi.it

† Electronic supplementary information (ESI) available: Synthesis and compound characterization, measurement details, additional spectra and graphics. See DOI: **https://doi.org/10.1039/d4tc01234h**

‡ These authors contributed equally.

Francesco Zinna earned his PhD in 2016 at the University of Pisa and then worked as a postdoctoral assistant at the University of Geneva. In 2018, he joined the faculty of the Department of Chemistry and Industrial Chemistry at the University of Pisa. Since the time of his master's thesis, his work has focused on developing chiral materials endowed with interesting chiroptical properties, with wide interests ranging from fundamental aspects to spectroscopic techniques and possible technological fallouts. In 2022 he was awarded the Ciamician Medal of the Italian Chemical Society for his contributions to the development of frontier chiroptical techniques.

Francesco Zinna

which was previously dominated by inorganic materials.[3–5] Introducing chirality in organic semiconductors opens the way to the fabrication of optoelectronic devices able to produce or detect circularly polarized (CP) light, such as CP-OLEDs[6–13] and CP-sensitive detectors,[14–18] as well as offers an intriguing approach to influence solid state aggregation.[2,19] Furthermore, chirality allows for the development of technologies to filter electrons based on their spin, thanks to the so-called chirality induced spin selectivity (CISS) effect.[20–25] CP-light finds applications in various contexts, including satellite communication and 5G technologies,[26] quantum optics,[27] security labelling,[28] bioimaging[29] and many advanced sensing technologies.[30,31] Such applications require a fast and reliable detection of circular polarization. This is generally possible through two different approaches: adopting optical elements or, alternatively, involving CP-sensitive materials.[32] The most classical example for the optical elements is represented by the coupling of a linear polarizer with a photoelastic modulator (PEM), which is generally employed to generate circular polarization in circular dichroism (both electronic, ECD, and vibrational, VCD) spectropolarimeters,[33,34] or its emission counterpart, namely circularly polarized luminescence (CPL).[35,36] Alternatively, the linear polarizer (LP) can be coupled with a static quarter-wave plate (QWP), both of them in the form of polymeric films.[37–39] Very recently, such a strategy has been adopted to physically separate and detect both circular polarizations, thanks to the further aid of a beam splitter.[40,41] This is not only confined to specialized applications, such as the ones mentioned above. In fact, in everyday life circular polarizers, made of coupled LP and QWP

films, are applied in front of the vast majority of displays, to prevent glare and obtain true black.[42] When involving chiral CP-sensitive materials, the most reliable setup for detecting CP-light is nowadays represented by CP-sensitive transistors.[32] They are characterized by good performances but, further than a CP-sensitive material, they also require an optimization of the device architecture, which is usually not trivial. Despite their fame as dyes and emitters,[43–47] chiral azole derivatives' chiroptical properties have never been investigated in thin films, but mainly in solution[48] or powder form.[49]

In the context of CP detection, one can distinguish between two extreme cases: accurate measurements of possibly weak signals on a full wavelength range *vs.* fast, inexpensive, miniaturizable detection of conspicuously polarized light. In the first case, one must resort to dedicated spectrofluoropolarimeters, based on PEM as CP-light modulators and photomultiplier tubes (PMT) as detectors. Such instruments can be extremely sensitive and accurate but at the cost of being very bulky (>1 linear meter) and expensive (>100 k€). On the other hand, several research groups addressed the latter challenge, developing cheap, compact and easy-to-use devices. To this end, static polarizing elements (QWP and LP) can replace the PEM,[50,51] while the detection could be operated by a CCD camera.[52–55] These set-ups can usually reliably record CPL signals with dissymmetry factors at least down to 10^{-2}.

A significant improvement could be the use of passive electronics as the detector, *i.e.* elements that do not need an external power to operate. An example of this principle is the photo-sensitive resistor (or photoresistor), widely employed in light-activated circuits. Anyway, such system is non-sensitive to light polarization.

In this work, we report the synthesis of four new 1-methyl-1*H*-imidazole-based chiral π-conjugated molecules and show their thin film chiroptical features (ECD and CPL). Moreover, we show that their CPL can also be measured

through an ultra-cheap setup based on a common photoresistor as the detector.

Results and discussion

Molecular design and synthesis

Chiral derivatives **1–4** (Scheme 1) were designed and synthesized to evaluate the effects of small structural variations on their supramolecular aggregation and the resulting chiroptical properties. Different supramolecular structures can be highlighted by chiroptical spectroscopies. For instance, the C-2 and C-5 positions of the central 1-methyl-1*H*-imidazole core are substituted with π-conjugated side-chains of similar nature, where the only difference is the presence or absence of a triple bond acting as a spacer (Scheme 1).

Compounds **1–4** were synthesized starting from commercially available 1-methyl-1*H*-imidazole. The synthetic strategy involved the functionalization of 1-methyl-1*H*-imidazole with distinct π-linkers *via* Pd-catalyzed cross-couplings.

The modular design of imidazole-based π-conjugated systems is outlined in Scheme S1 (ESI†). Symmetrical 2,5-diaryl and dialkynyl-substituted imidazoles **1** and **4** were prepared *via* two-fold Pd-catalyzed cross-coupling reactions. In detail, compound **1** was synthesized by one-pot Pd-catalyzed and Cu-assisted direct arylation on 1-methyl-1*H*-imidazole with 4-bromobenzaldehyde.[56] Conversely, compound **4** was obtained by a C-2/C-5 regioselective iodination, followed by a two-fold alkynylation under classical Sonogashira conditions.[57,58]

Asymmetrical 2,5-disubstituted imidazoles **2** and **3** were prepared in a stepwise fashion, taking advantage of C-5 or C-2 regioselective cross-coupling reactions. For the synthesis of **2**, a C-5 regioselective Pd-catalyzed direct arylation was firstly performed on 1-methyl-1*H*-imidazole, followed by a Pd-catalyzed dehydrogenative alkynylation at the C-2 position.[59,60] Finally,
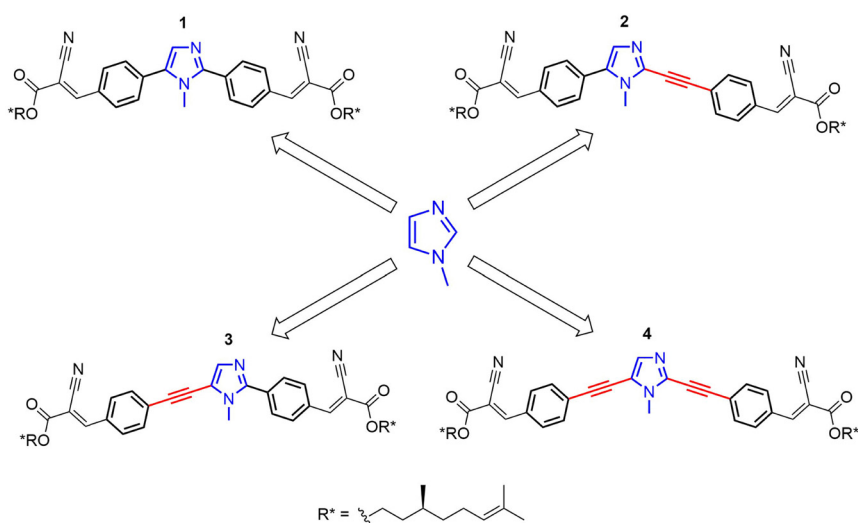
Scheme 1 Schematic representation of the structures of chiral π-conjugated derivatives obtained from 1-methyl-1*H*-imidazole and investigated in this work. The central π-conjugated cores (bold bonds) differ in the presence or absence of triple bonds in between aryl groups and positions C-2 and/or C-5 of the central moiety.

This journal is © The Royal Society of Chemistry 2024

J. Mater. Chem. C, 2024, **12**, 9210–9216 | **9211**

compound **3** was prepared *via* a Pd- and Cu-assisted C-2 direct arylation on 1-methyl-1*H*-imidazole,[61] followed by alkynylation at the C-5 position with 4-ethynylbenzaldehyde through a one-pot bromination and Sonogashira coupling procedure.[62]

The chiral aliphatic chain, derived from β-citronellol,[2] was introduced in the last step of each synthesis *via* Knoevenagel condensation (Scheme S1, ESI†).[63,64]

Material characterization

We started the characterization of the four chiral 1-methyl-1*H*-imidazole-based dyes **1–4** with their optical properties in solution. The normalized UV-vis absorption and photoluminescence (PL) emission spectra in CHCl$_3$ are reported in Fig. S1 (ESI†). All the compounds showed a main absorption band with similar broadening between 340 nm and 460 nm. A slight red-shift of maximum absorption can be observed going from compound **1** to compound **4**, which can be rationalized with the increased conjugation ensured by the presence of triple bonds. Interestingly, PL spectra of Fig. S1 (ESI†) show that compounds **2–4** show similar elevated Stokes shifts of around 140 nm (6200 cm^{-1}), while compound **1** is characterized by a smaller Stokes shift of about 100 nm (5000 cm^{-1}), associable to a decreased polarity of the excited state. These Stokes shifts are in the typical range for imidazole-based systems.[65] It is important to note that no significant ECD or CPL has been observed in the solution.

The thin film characterization started with the investigation of the optical and chiroptical properties. Thin films of all compounds were prepared by spin-coating and solvent annealed with CH$_2$Cl$_2$ vapours. Films prepared by molecules **1**/**2** showed blue-shifted main absorption bands (Fig. 1), if compared with the solution absorption (Fig. S1, ESI†). On the contrary, thin films of **3**/**4** are characterized by red-shifted main absorption bands (Fig. 1) with respect to the solution (Fig. S1, ESI†).

Interestingly, small structural variations between the compounds investigated are associated to considerable changes in the magnitude, form and origin of the chiroptical properties of the solid-state aggregates. In fact, thin films formed by compounds **2**/**4** showed much less pronounced ECD properties than compounds **1**/**3** (Fig. 1(a) and(b)). A useful metric to quantify the ECD independently from the film thickness is represented by the absorption *g*-factor ($g_{abs} = \Delta A/A$).[2] Thin films of compounds **1**/**3** showed maximum g_{abs} values (−0.34 at 529 nm and −0.17 at 521 nm, respectively, Fig. S2b, ESI†) of more than one order of magnitude higher than the ones of molecules **2**/**4** (+0.008 around 530 nm at −0.007 at 408 nm, respectively, Fig. S2a, ESI†). By structurally comparing molecules **2** and **3** (Scheme 1), one can notice that switching atoms in positions 3 and 4 of the central imidazole core leads to the interconversion of one chemical structure into the other, and *vice versa*. Such single-atom-switching, which is a minor structural modification, deeply affects the final chiroptical properties in thin films, as already discussed. Focusing on spectral features, compound **1** shows a bisignate ECD signal between 460 nm and 320 nm, with a crossover point at 373 nm almost coincidental with the absorption maximum (381 nm). Of note and rarely observed, is a marked absorption blue shift (16 nm, 1000 cm^{-1}) from the solution to the aggregate. This is consistent with an exciton coupling with a coupling potential approx. 1730 cm^{-1}, formed between interacting monomers forming an H-type aggregate with right-handed helicity. On the other hand, the seemingly similar bisignate band displayed by compound **3** is not consistent with an excitonic feature, as the apparent exciton potential of 5600 cm^{-1} would be far too large. Moreover, the
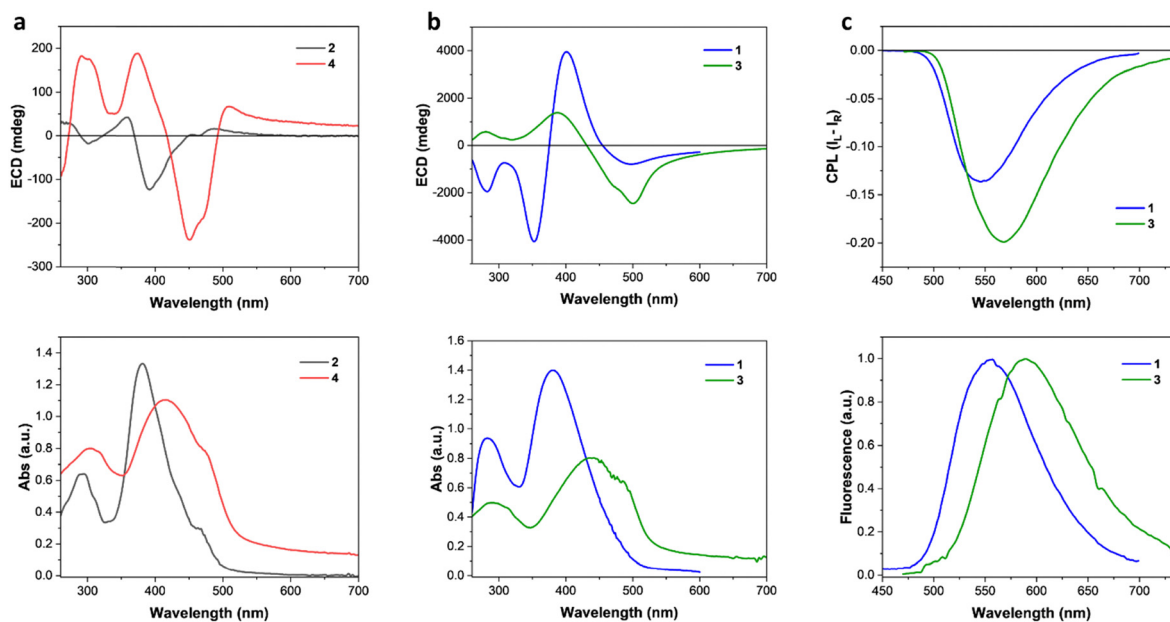

Fig. 1 ECD (top) and absorption (bottom) spectra in thin films of a couple of compounds (a) **2**/**4** and (b) **1**/**3**. (c) CPL (top) measured with a benchtop spectrofluoropolarimeter and fluorescence (bottom) spectra of compounds **1**/**3**.

9212 | *J. Mater. Chem. C*, 2024, **12**, 9210–9216

This journal is © The Royal Society of Chemistry 2024

crossover point does not match with the absorption maximum, while the positive ECD band at 392 nm lies in correspondence to $S_0 \rightarrow S_2$ transition, as shown by TD-DFT calculations (ESI†). The spectral features would therefore suggest a molecular origin of the ECD signals, rather than an excitonic one, stemming from a rigidification of the molecules in the aggregate, each adopting a twisted conformation. In this case a red-shift of the absorption band from solution to the aggregate is consistent with an overall head-to-tail arrangement (J-type aggregate) in addition to solid-state planarization on the phenylethynyl side.[66] In both cases, the exceptionally large ellipticity values are likely related to electric-magnetic couplings between closely packed and twisted chromophores.[67] The presence of a direct 2-imidazolyl-phenyl junction (as in 1 and 3) seems crucial to impart the proper twist to establish such kinds of interactions, while the ethynyl bridge (as in 2 and 4) would favour a more planar structure reducing the intrinsic magnetic transition moment. It is worth mentioning that while several aggregate systems with exceptionally high dissymmetry factors are known to date, a conclusive interpretation of the phenomenon is still missing.[68]

Given the highly intense ECD characterizing thin films of compounds 1/3 and the observation of a remarkable solid-state fluorescence, CPL measurements were carried out using a benchtop spectrofluoropolarimeter.[69] Compound 1 in thin film showed an intense negative CPL signal at 550 nm, while molecule 3 showed a negative signal of slightly higher intensity around 570 nm (Fig. 1(c)). Compound 3 showed a luminescence dissymmetry factor (g_{lum}) value of -0.32, twice the value of -0.16 obtained for the film of molecule 1 (Fig. S3, ESI†). Such g_{lum} values are among the highest ever observed for thin films made of small organic chiral molecules and on the same order of magnitude of thin films prepared with luminescent polymers with chiral dopants.[2,70] Films of compounds 2 and 4 showed only a vanishingly small CPL ($|g_{lum}| < 10^{-3}$, Fig. S5, ESI†). The impact of film thickness (ranging approximately from 100 to 400 nm) on the ECD and CPL was investigated. In the case of 3, films up to 100 nm did not show significant chiroptical properties, while films of 150 nm or higher displayed similar ECD and CPL features. Both the normalized ECD and CPL intensities increase slightly but significantly with thickness (Fig. S7, ESI†).

Morphological analyses (optical microscopy, scanning electron microscopy and atomic force microscopy) of thin films showed that stronger chiroptical properties are associated with the presence of ordered phases on the relative films. Cross-polarized microscopy allowed for the identification of birefringent domains for thin films of 1 and especially 3 (Fig. S8, ESI†). In particular, the thin film of 1 is composed by birefringent spots of around 1 μm in an environment majorly dominated by an amorphous area (Fig. S8b, ESI†). The thin film of 3 is fully dominated by a birefringent ordered phase (Fig. S8d, ESI†), while no birefringent domains are observed for films of 2 and 4. Scanning electron microscopy (SEM) further highlighted what was observed by cross-polarized microscopy (Fig. S11, ESI†). The film of compound 3 shows a reticular structure, made of fibrillar/dendritic patterns, at sub 10 μm scale (Fig. S11c and d,

ESI†), as observed by SEM and AFM. Such structures form island-like domains, possibly responsible for the birefringent patterns observed in cross-polarized microscopy. In contrast with the textures observed for films of 1 and 3, films of 2 and 4 show a mostly amorphous surface characterized by closely spaced holes (Fig. S10 and S12, ESI†). The AFM analysis also allowed for a coarse estimation of the film thickness, of approximately 200 nm in every case (Fig. S14, ESI†), as well as surface roughness (calculated as root mean square, RMS) ranging from 36 to 99 nm. Finally, thanks to circularly polarized microscopy (CPM)[38] we were able to map the spatially resolved ECD of the film of 3 at 500 nm. CPM images highlighted a generally negative ECD activity and dissymmetry factor over an area of around 3 mm^2 (Fig. S15, ESI†). The g_{abs} factor is normally distributed around -0.15 (Fig. S16, ESI†), consistent with the ECD spectrum reported in Fig. 1. The presence of domains or clusters with significantly different ECD was not observed.

Measuring CPL through an ultra-cheap setup

Given the considerably intense CPL given by compound 3 in thin film, we designed an ultra-cheap instrumental setup dedicated to its detection. The components of this setup are reported in Fig. 2(a). Thanks to an in-line geometry, a UV LED centred at 365 nm excites the photoluminescence of the sample. The luminescence is isolated into its circularly polarized contributions through a cheap circular polarizer filtering the desired handedness of light. After this, the light is restricted to a defined spectral range by a bandpass filter. This component has two functions: allowing for a modest spectral resolution and avoiding the visible component of the UV LED to reach the detector. Finally, the circularly polarized light emitted from the sample is revealed using an ultra-cheap (<1 €) photoresistor, which passively detects the incident light intensity as a function of the resistance (R), measured with a multi-purpose digital multimeter operated in ohmmeter mode. The photoresistor conductance ($G = 1/R$) was confirmed to be linearly proportional to the light intensity (Fig. S17, ESI†). In this way, the left and right circular components of the emission can be collected independently by changing the circular polarizer. The g_{lum} can be calculated as:

$$g_{lum} = 2\frac{\dfrac{1}{R_L} - \dfrac{1}{R_R}}{\dfrac{1}{R_L} + \dfrac{1}{R_R}}$$

where R_L and R_R are the resistance values measured with left and right circular polarizers.

To test the setup, we validated it *via* measurements of known compounds. To this end, we chose CsEu(hfbc)$_4$ (hfbc = heptafluorobutyrylcamphorate, see ESI†), widely known for its remarkable CPL.[71,72] By applying a narrow bandpass filter centred at 590 nm, the CPL of the $^5D_0 \rightarrow {}^7F_1$ transition of CsEu(hfbc)$_4$ was measured, finding g_{lum} values of $+1.30$ (st. dev. = 0.011) for CsEu((+)hfbc)$_4$ and -1.30 (st. dev. = 0.011) for CsEu((−)hfbc)$_4$ (Table S1, ESI†), in good agreement with the values reported in
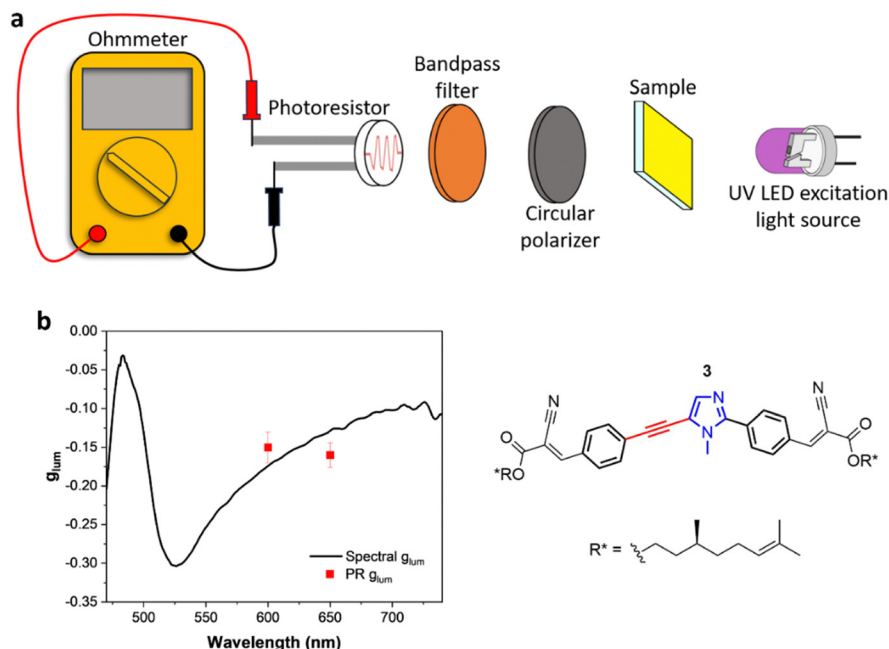
Fig. 2 (a) Experimental setup of optical and electronic components involved in ultra-cheap CPL detection. (b) Graphical representation of g_{lum} values obtained through photoresistor detection (PR g_{lum}) in comparison with the spectral g_{lum} obtained with a standard benchtop CPL spectropolarimeter. The error bars reported for the PR g_{lum} values represent the standard deviation over a set of measurements.

the literature.[71–73] Furthermore, we measured a CPL-inactive fluorescent achiral material (fluorescein solution) as a blank, to define the minimum detectable $|g_{lum}|$. In this way we determined the limit of $|g_{lum}|$ detection as approximately 0.02, which was defined as 3 times the standard deviation over a set of multiple measurements of the blank (fluorescein solution, Table S1, ESI†). Following these first validations, this ultra-cheap CPL setup was adopted in the CPL characterization of films of compound **3**, focusing on two specific wavelengths (600 nm and 650 nm) selected with two different bandpass filters. The values of −0.15 (st. dev. = 0.020) and −0.16 (st. dev. = 0.016) obtained, respectively, with the bandpass filter centered at 600 nm and 650 nm appear in good agreement with the expected g_{lum}, as measured with a standard benchtop spectrofluoropolarimeter (Fig. 2(b)). These results highlight the possibility to detect the CPL of thin films just by the aid of inexpensive optic elements and a photoresistor as the detector, instead of using expensive instruments and electronically sophisticated photomultiplier tubes.[74]

Conclusions

In summary, in this work we have reported the synthesis and the thin film investigation of four 1-methyl-1H-imidazole chiral derivatives, differing by small structural variations among them. In particular, we have shown how tiny structural variations (such as, for example, the single-atom-switch between compounds **2** and **3**) lead to significant modifications of the chiroptical properties magnitude. Furthermore, the aggregate type (H $vs.$ J-type) and the origin of the chiroptical activity are affected by minor structural modifications, as established for

molecules **1/3**. Finally, we showed that the bright CPL of films of compound **3** can be detected with an unprecedented ultra-cheap setup based on passive detection.

Conflicts of interest

There are no conflicts to declare.

Acknowledgements

References

1 J. Crassous, M. J. Fuchter, D. E. Freedman, N. A. Kotov, J. Moon, M. C. Beard and S. Feldmann, *Nat. Rev. Mater.*, 2023, **8**, 365–371.
2 G. Albano, G. Pescitelli and L. Di Bari, *Chem. Rev.*, 2020, **120**, 10145–10243.
3 J. M. Nassar, J. P. Rojas, A. M. Hussain and M. M. Hussain, *Extreme Mech. Lett.*, 2016, **9**, 245–268.
4 J. Song, X. Feng and Y. Huang, *Natl. Sci. Rev.*, 2016, **3**, 128–143.

5 Y. Sun and J. A. Rogers, *Adv. Mater.*, 2007, **19**, 1897–1916.

6 Y. Zhang, T. Jing, Y. Quan, S. Ye and Y. Cheng, *Adv. Opt. Mater.*, 2022, **10**, 2200915.

7 G. Albano, L. A. Aronica, A. Minotto, F. Cacialli and L. Di Bari, *Chem. – Eur. J.*, 2020, **26**, 16622–16627.

8 L. Wan, Y. Liu, M. J. Fuchter and B. Yan, *Nat. Photonics*, 2023, **17**, 193–199.

9 L. Wan, J. Wade, X. Shi, S. Xu, M. J. Fuchter and A. J. Campbell, *ACS Appl. Mater. Interfaces*, 2020, **12**, 39471–39478.

10 X. Zhang, Z. Xu, Y. Zhang, Y. Quan and Y. Cheng, *J. Mater. Chem. C*, 2020, **8**, 15669–15676.

11 Y. Yang, R. C. Da Costa, D. M. Smilgies, A. J. Campbell and M. J. Fuchter, *Adv. Mater.*, 2013, **25**, 2624–2628.

12 L. Wan, J. Wade, F. Salerno, O. Arteaga, B. Laidlaw, X. Wang, T. Penfold, M. J. Fuchter and A. J. Campbell, *ACS Nano*, 2019, **13**, 8099–8105.

13 F. Furlan, J. M. Moreno-Naranjo, N. Gasparini, S. Feldmann, J. Wade and M. J. Fuchter, *Nat. Photonics*, 2024, DOI: **10.1038/s41566-024-01408-z**.

14 Y. Yang, R. C. da Costa, M. J. Fuchter and A. J. Campbell, *Nat. Photonics*, 2013, **7**, 634–638.

15 J. Cheng, F. Ge, C. Zhang, Y. Kuai, P. Hou, Y. Xiang, D. Zhang, L. Qiu, Q. Zhang and G. Zou, *J. Mater. Chem. C*, 2020, **8**, 9271–9275.

16 C. Zhang, X. Wang and L. Qiu, *Front. Chem.*, 2021, **9**, 711488.

17 L. Zhang, I. Song, J. Ahn, M. Han, M. Linares, M. Surin, H.-J. Zhang, J. Hak Oh and J. Lin, *Nat. Commun.*, 2021, **12**, 142.

18 W. Shi, F. Salerno, M. D. Ward, A. Santana-Bonilla, J. Wade, X. Hou, T. Liu, T. J. S. Dennis, A. J. Campbell, K. E. Jelfs and M. J. Fuchter, *Adv. Mater.*, 2021, **33**, 2004115.

19 J. Wade, F. Salerno, R. C. Kilbride, D. K. Kim, J. A. Schmidt, J. A. Smith, L. M. LeBlanc, E. H. Wolpert, A. A. Adeleke, E. R. Johnson, J. Nelson, T. Mori, K. E. Jelfs, S. Heutz and M. J. Fuchter, *Nat. Chem.*, 2022, **14**, 1383–1389.

20 R. Naaman and D. H. Waldeck, *J. Phys. Chem. Lett.*, 2012, **3**, 2178–2187.

21 V. Kiran, S. P. Mathew, S. R. Cohen, I. Hernández Delgado, J. Lacour and R. Naaman, *Adv. Mater.*, 2016, **28**, 1957–1962.

22 P. C. Mondal, N. Kantor-Uriel, S. P. Mathew, F. Tassinari, C. Fontanesi and R. Naaman, *Adv. Mater.*, 2015, **27**, 1924–1927.

23 R. Rodríguez, C. Naranjo, A. Kumar, P. Matozzo, T. K. Das, Q. Zhu, N. Vanthuyne, R. Gómez, R. Naaman, L. Sánchez and J. Crassous, *J. Am. Chem. Soc.*, 2022, **144**, 7709–7719.

24 A. Privitera, E. Macaluso, A. Chiesa, A. Gabbani, D. Faccio, D. Giuri, M. Briganti, N. Giaconi, F. Santanni, N. Jarmouni, L. Poggini, M. Mannini, M. Chiesa, C. Tomasini, F. Pineider, E. Salvadori, S. Carretta and R. Sessoli, *Chem. Sci.*, 2022, **13**, 12208–12218.

25 B. P. Bloom, Y. Paltiel, R. Naaman and D. H. Waldeck, *Chem. Rev.*, 2024, **124**, 1950–1991.

26 K. M. Mak, H. W. Lai, K. M. Luk and C. H. Chan, *IEEE Access*, 2014, **2**, 1521–1529.

27 J. F. Sherson, H. Krauter, R. K. Olsson, B. Julsgaard, K. Hammerer, I. Cirac and E. S. Polzik, *Nature*, 2006, **443**, 557–560.

28 L. E. MacKenzie and R. Pal, *Nat. Rev. Chem.*, 2020, **5**, 109–124.

29 V. V. Tuchin, *J. Biomed. Photonics Eng.*, 2015, 3.

30 S.-S. Lin, K. M. Yemelyanov, E. N. Pugh and N. Engheta, in IEEE International Conference on Networking, Sensing and Control, 2004, IEEE, pp. 216–221.

31 J. S. Tyo, M. P. Rowe, E. N. Pugh and N. Engheta, *Appl. Opt.*, 1996, **35**, 1855–1870.

32 X. Shang, L. Wan, L. Wang, F. Gao and H. Li, *J. Mater. Chem. C*, 2022, **10**, 2400–2410.

33 J. C. Cheng, L. A. Nafie and P. J. Stephens, *J. Opt. Soc. Am.*, 1975, **65**, 1031–1035.

34 A. F. Drake, *J. Phys. E*, 1986, **19**, 170–181.

35 I. Z. Steinberg and A. Gafni, *Rev. Sci. Instrum.*, 1972, **43**, 409–413.

36 G. Longhi, E. Castiglioni, J. Koshoubu, G. Mazzeo and S. Abbate, *Chirality*, 2016, **28**, 696–707.

37 K. Claborn, E. Puklin-Faucher, M. Kurimoto, W. Kaminsky and B. Kahr, *J. Am. Chem. Soc.*, 2003, **125**, 14825–14831.

38 A. Taddeucci, F. Zinna, G. Siligardi and L. Di Bari, *Chem. Biomed. Imaging*, 2023, **1**, 471–478.

39 J. P. Riehl and F. S. Richardson, *Circularly Polarized Luminescence Spectroscopy*, 1986, vol. 86.

40 L. E. MacKenzie, L.-O. Pålsson, D. Parker, A. Beeby and R. Pal, *Nat. Commun.*, 2020, **11**, 1676.

41 P. Stachelek, L. MacKenzie, D. Parker and R. Pal, *Nat. Commun.*, 2022, **13**, 553.

42 B. C. Kim, Y. J. Lim, J. H. Song, J. H. Lee, K.-U. Jeong, J. H. Lee, G.-D. Lee and S. H. Lee, *Opt. Express*, 2014, **22**, A1725.

43 Y. A. Son, B. S. Kim, M. S. Choi and S. H. Kim, *Mol. Cryst. Liq. Cryst.*, 2009, **498**, 158–164.

44 M. Saleem and K. H. Lee, *J. Fluoresc.*, 2015, **25**, 217–226.

45 P. T. Chou and Y. Chi, *Chem. – Eur. J.*, 2007, **13**, 380–395.

46 F. Bellina, C. Manzini, G. Marianetti, C. Pezzetta, E. Fanizza, M. Lessi, P. Minei, V. Barone and A. Pucci, *Dyes Pigm.*, 2016, **134**, 118–128.

47 G. Marianetti, M. Lessi, V. Barone, F. Bellina, A. Pucci and P. Minei, *Dyes Pigm.*, 2018, **157**, 334–341.

48 D. W. Miles, G. R. Revankar and R. K. Robins, *J. Phys. Chem.*, 1983, **87**, 2444–2450.

49 H. Liu, D.-D. Ren, P.-F. Gao, K. Zhang, Y.-P. Wu, H.-R. Fu and L.-F. Ma, *Chem. Sci.*, 2022, **13**, 13922–13929.

50 F. Zinna, M. Pasini, F. Galeotti, C. Botta, L. Di Bari and U. Giovanella, *Adv. Funct. Mater.*, 2017, **27**, 1603719.

51 O. G. Willis, F. Petri, G. Pescitelli, A. Pucci, E. Cavalli, A. Mandoli, F. Zinna and L. Di Bari, *Angew. Chem., Int. Ed.*, 2022, **61**, e202208326.

52 D. F. De Rosa, P. Stachelek, D. J. Black and R. Pal, *Nat. Commun.*, 2023, **14**, 1537.

53 B. Baguenard, A. Bensalah-Ledoux, L. Guy, F. Riobé, O. Maury and S. Guy, *Nat. Commun.*, 2023, **14**, 1065.

54 L. E. MacKenzie, L.-O. Pålsson, D. Parker, A. Beeby and R. Pal, *Nat. Commun.*, 2020, **11**, 1676.

55 P. Stachelek, L. MacKenzie, D. Parker and R. Pal, *Nat. Commun.*, 2022, **13**, 553.

This journal is © The Royal Society of Chemistry 2024

J. Mater. Chem. C, 2024, **12**, 9210–9216 | **9215**

56 M. Lessi, G. Panzetta, G. Marianetti and F. Bellina, *Synthesis*, 2017, 4676–4686.

57 K. G. Holden, M. N. Mattson, K. H. Cha and H. Rapoport, *J. Org. Chem.*, 2002, **67**, 5913–5918.

58 M. Toba, T. Nakashima and T. Kawai, *Macromolecules*, 2009, **42**, 8068–8075.

59 F. Bellina, S. Cauteruccio, A. Di Fiore, C. Marchetti and R. Rossi, *Tetrahedron*, 2008, **64**, 6060–6072.

60 F. Bellina, M. Biagetti, S. Guariento, M. Lessi, M. Fausti, P. Ronchi and E. Rosadoni, *RSC Adv.*, 2021, **11**, 25504–25509.

61 G. Del Frate, F. Bellina, G. Mancini, G. Marianetti, P. Minei, A. Pucci and V. Barone, *Phys. Chem. Chem. Phys.*, 2016, **18**, 9724–9733.

62 F. Bellina, M. Lessi, G. Marianetti and A. Panattoni, *Tetrahedron Lett.*, 2015, **56**, 3855–3857.

63 H. B. Tukhtaev, K. L. Ivanov, S. I. Bezzubov, D. A. Cheshkov, M. Ya Melnikov and E. M. Budynina, *Org. Lett.*, 2019, **21**, 1087–1092.

64 M. Nahmany and A. Melman, *Org. Lett.*, 2001, **3**, 3733–3735.

65 J. Jayabharathi, V. Thanikachalam, N. Srinivasan and M. Venkatesh Perumal, *Spectrochim. Acta, Part A*, 2012, **90**, 125–130.

66 F. Babudri, D. Colangiuli, L. Di Bari, G. M. Farinola, O. Hassan Omar, F. Naso and G. Pescitelli, *Macromolecules*, 2006, **39**, 5206–5212.

67 B. Laidlaw, J. Eng, J. Wade, X. Shi, F. Salerno, M. J. Fuchter and T. J. Penfold, *Chem. Commun.*, 2021, **57**, 9914–9917.

68 J. L. Greenfield, J. Wade, J. R. Brandt, X. Shi, T. J. Penfold and M. J. Fuchter, *Chem. Sci.*, 2021, **12**, 8589–8602.

69 F. Zinna, T. Bruhn, C. A. Guido, J. Ahrens, M. Bröring, L. Di Bari and G. Pescitelli, *Chem. – Eur. J.*, 2016, **22**, 16089–16098.

70 Y. Yang, R. C. da Costa, D. Smilgies, A. J. Campbell and M. J. Fuchter, *Adv. Mater.*, 2013, **25**, 2624–2628.

71 J. L. Lunkley, D. Shirotani, K. Yamanari, S. Kaizaki and G. Muller, *Inorg. Chem.*, 2011, **50**, 12724–12732.

72 J. L. Lunkley, D. Shirotani, K. Yamanari, S. Kaizaki and G. Muller, *J. Am. Chem. Soc.*, 2008, **130**, 13814–13815.

73 F. Zinna, U. Giovanella and L. Di Bari, *Adv. Mater.*, 2015, **27**, 1791–1795.

74 B. K. Lubsandorzhiev, *Nucl. Instrum. Methods Phys. Res., Sect. A*, 2006, **567**, 236–238.